STM JOURNALS

Journal of
Polymer & Composites

ISSN: 2321-2810 (Online)
ISSN: 2321-8525 (Print)
Volume 13, Special Issue 1, 2025
DOI (Journal): 10.37591/JoPC

https://journals.stmjournals.com/jopc

Research JoPC

Simplified Solution to Analysis Risk Assessment of Reinforcement type Soil Wall Considering Seismic Waves with Uniform Surcharge

Niranjan Singh[1,*], Ashish Gupta[2]

Abstract

Due to failure of reinforced soil wall in various country the various risk factor are associated to these failure. In the present pseudo-static analysis some risk factor analysis have been done by considering the seismic waves with uniform surcharge and also consider surcharge's inertial behavior at risk factor of horizontal and vertical coefficients of accelerations at k_h = 0.24, 0.36 and k_v = 0.12, 0.18 taking into account. The earlier studies mostly utilized the normalised tensile reinforcing force for reinforced soil walls' seismic stability backfilled with cohesive soil employing some demanding methods taking into account the pseudo-static seismic forces. Reinforced soil wall are chemically composed with reinforcement and concrete of appropriate grade. Reinforcement type soil wall are Hybrid Composite Material structure

Keywords: Risk assessment, reinforced soil wall, seismic waves, uniform surcharge, hybrid composite materials

INTRODUCTION

Reinforced soil walls are currently employed as an alternative to traditional concrete retaining walls to support the soil fills in civil infrastructure projects. This is because it can be built quickly, cheaply, and easily demolished, and doesn't require substantial work. Because reinforced walls are almost vertical, less space is needed. This method works well in metropolitan areas with constrained ground space and difficulty functioning while minimizing traffic disruption. Previously, the retaining wall design based on static analysis on Coulomb's, Rankine's theories of earth pressure. However, numerous scholars made considerable attempts utilizing the pseudo-static approach due to the necessity of building the soil wall in a seismically active area such as A. Gupta and V. A. Sawant, 'Simplified solution to analyse seismic stability of reinforced soil wall'[1]. V. K. Chandaluri, V. A. Sawant, and S. K. Shukla, 'Seismic Stability Analysis of Reinforced Soil Wall Using Horizontal Slice Method'[2]. M. Ahmadabadi and A. Ghanbari, 'New procedure for active earth pressure calculation in retaining walls with reinforced cohesive-frictional backfill'[3]. E. Guler, M. Hamderi, and M. M. Demirkan, 'Numerical analysis of reinforced soil-retaining wall structures with cohesive and granular backfills'[4]. H. I. Ling, D. Leshchinsky, and E. B. Perry, 'Seismic design and performance of geosynthetic-reinforced soil structures'[5]. H. Nouri, A. Fakher, and C. J. F. P. Jones, 'Development of Horizontal Slice Method for seismic stability analysis of reinforced slopes and walls'[6]. D. Choudhury and S. S. Nimbalkar, 'Pseudo-dynamic approach of seismic active earth pressure behind retaining wall'[7]. R. K. Rowe and

***Author for Correspondence**
Niranjan Singh

[1]Research Scholar, Department of Civil Engineering, Bundelkhand Institute of Engineering and Technology Jhansi, Uttar Pradesh, India
[2]Associate Professor, Department of Civil Engineering, Bundelkhand Institute of Engineering and Technology Jhansi, Uttar Pradesh, India

Received Date: April 23, 2024
Accepted Date: July 01, 2024
Published Date: December 17, 2024

Citation: Niranjan Singh, Ashish Gupta. Simplified Solution to Analysis Risk Assessment of Reinforcement type Soil Wall Considering Seismic Waves with Uniform Surcharge. Journal of Polymer & Composites. 2025; 13(Special Issue 1): S452–S458p.

© STM Journals 2025. All Rights Reserved

K. L. Soderman, 'Approximate Method for Estimating the Stability of Geotextile-Reinforced Embankments.[8]. B. M. Basha and P. K. Basudhar, 'Pseudo Static Seismic Stability Analysis of Reinforced Soil Structures'[9]. S. Ghosh and R. Prasad Sharma, 'Seismic Active Earth Pressure on the Back of Battered Retaining Wall Supporting Inclined Backfill'[10]. Various scenario of failure of reinforced soil wall are analysis are shown in Figures. 1(a & b). The chemical composition of reinforcement type soil wall is reinforcement, concrete, cement, sand. the material composition of reinforcement type soil wall have different chemical properties. While constructing the reinforcement type soil wall of particular grade chemical reaction between cement and water take place after adding the water Bonding of materials stand after this chemical reaction. Types of failure that are taken into consideration are Overturning, Sliding, Bearing Failure of Soil, Slope Stability Failures.

Figure 1. Various scenario of reinforced soil wall failure (a) Nepal earthquake in 2015 (Okamura et al., 2015) (b) Gorkha Nepal earthquake in 2015 (Chiaro et al., 2015)

Analytical Solution

Figure 2 depicts a reinforced earth wall (AC) with a height of H backfilled with c-ϕ soil that is subject to a $q/$ m length of surcharge. W_s are the weight of the active trial failure assumption (ABC) wedge and further, this system's numerous forces are depicted in Figure.2. C is the unit Cohesion and ϕ is the frictional resistance angle. In this study, the retaining wall's backfilled side is assumed to be vertical. It is believed that the plane of failure runs together AB and makes a α angle relative to the horizontal, which passes via A point. The reinforced soil wedge is being subjected to seismic forces of inertia in both vertical and horizontal directions that are $k_h.W_s$ and $k_v.W_s$, and surcharge's inertial impact $k_h.q$ and $k_v.q$ is also taken where k_h and k_v are the seismic coefficients the major risk factor and these in horizontal

© STM Journals 2025. All Rights Reserved

and vertical directions. When oriented downward, the risk factor (k_v) is considered positive. On the failure plane AB, the entire cohesive force is expressed as $C = cH\,cosec\alpha$. On the failure plane AB, The normal force is N, and the shear force is T. The normal forces and shear, T and N combine to form the resultant force of magnitude F. T_i is the necessary strength of i_{th} layer of reinforcement. The value n represents the total number of reinforcing layers.

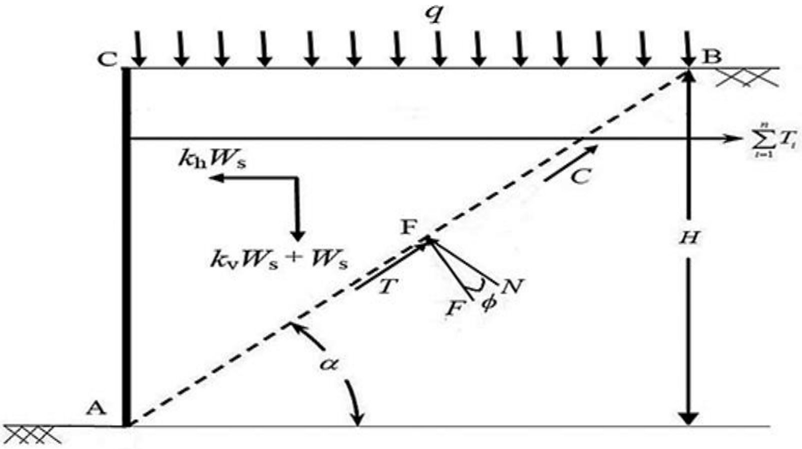

Figure 2. Forces acting on a reinforced soil wall with a c–φ soil fill.

Consider the acting forces on reinforced soil wall are in equilibrium in vertical and horizontal directions to find out the reinforcement force coefficient K.

$$K = \frac{\left[\begin{array}{l}-C^* \tan^2\alpha + \left(1 + k_h \tan\phi + k_v + k_h q^* \tan\phi + k_v q^*\right)\tan\alpha \\ + \left(k_h - k_v \tan\phi - k_v q^* \tan\phi - C^* + k_h q^* - \tan\phi\right)\end{array}\right]}{\left(\tan\alpha + \tan^2\alpha \tan\phi\right)} \quad (1)$$

To obtain the (α_{CR}) of the failure plane, partially differentiate Eqn. (1) with respect to α.

$$\frac{\partial K}{\partial \alpha} = 0 \quad (2)$$

$$\begin{array}{l}A^* \tan^2\alpha + B^* \tan\alpha + D^* = 0 \\ where,\ A^* = \left(k_h \tan^2\phi + k_v \tan\phi + C^* + \tan\phi + k_h q^* \tan^2\phi + k_v q^* \tan\phi\right) \\ B^* = \left[2k_h \tan\phi - 2k_v \tan^2\phi - 2\tan\phi\left(C^* + \tan\phi\right) - 2k_v q^* \tan^2\phi + 2k_h q^* \tan\phi\right] \\ D^* = \left(k_h - k_v \tan\phi - C^* - k_v q^* \tan\phi + k_h q^* - \tan\phi\right)\end{array} \quad (3)$$

On solving Eqn. (3), failure plane's critical inclination can be represented as:

$$\alpha = \alpha_{CR} = \tan^{-1}\left(\frac{-B^* \pm \sqrt{\left(B^{*2} - 4A^* D^*\right)}}{2A^*}\right) \quad (4)$$

Using $\alpha = \alpha_{CR}$ value in Eqn. (1), K_{max} can be calculated as:

$$K_{max} = \frac{\left[\begin{array}{l}-C^* \tan^2\alpha_{CR} + \left(\begin{array}{l}1 + k_h \tan\phi + k_v \\ + k_h q^* \tan\phi + k_v q^*\end{array}\right)\tan\alpha_{CR} \\ + \left(k_h - k_v \tan\phi - k_v q^* \tan\phi - C^* + k_h q^* - \tan\phi\right)\end{array}\right]}{\left(\tan\alpha_{CR} + \tan^2\alpha_{CR} \tan\phi\right)} \quad (5)$$

RESULTS AND DISCUSSION

With reference to generalized Eqns. (4 and 5) for calculating the (α_{CR}) of the plane of failure and the total strength of reinforcement required (K_{max}), parametric analysis is done. The geometric

© STM Journals 2025. All Rights Reserved

specifications of the reinforced soil wall and the attributes of soil backfill are, k_h = 0.24, 0.36 and k_v = 0.12, 0.18; without dimensions soil cohesion (c^*) = 0, 0.33330; without dimensions surcharge (q^*) = 0.55560 and 1.1110; frictional resistance angle (ϕ) = 20°, 25°, 30°, 35°, 40° and 45°.

Impacts of k_h, k_v, q on K_{max}Variation of K_{max}

with (k_h = 0.24, 0.36 and k_v = 0.12, 0.18) for different angles of frictional resistance ϕ = 20°, 25°, 30°, 35°, 40°, 45°) are shown in Figures. (3-6)for reinforced soil wall. The dimensionless cohesion of soil (c^* = 0.33330) and dimensionless loading of surcharge (q^* = 0.55560, 1.1110) are depicted in the design figures. In Figure. (3-6) as seismic coefficients both vertically and horizontally are increases, the reinforcement strength requirement increases in order to maintain the stability of reinforced soil walls in seismic condition.

The impact of k_h and k_v be dependent on the loading of surcharge and cohesion of soil values. Figs. (3-6) compare the reinforcement force maximum values K_{max}. In the soil backfill with cohesion for surcharge (q^*= 0.55560, 1.1110), respectively. It is clear that the necessary K_{max} rises with rise in k_v and loading of surcharge. As an example, for the case of (c^* = 0.33330, q^* = 0.55560) (Figs. 3-4), the necessary K_{max} at (k_h = 0.24 and k_v = 0.12) is 0.1449 for angle of frictional resistance equal to 30°. With changes in k_h from 0.24 to 0.36, increase in K_{max} is 57.97%. In a similar way, for the changes in surcharge (q^* = 0.55560 to 1.1110) (Figs. 5-6), the essential K_{max} increased by 29.12%. It is obvious that the impact of the surcharge is greater since it significantly affects the lateral earth pressure. It can be inferred that while analysing the reinforced soil wall in seismic conditions, the impacts of k_h is significantly more than the impact of k_v.

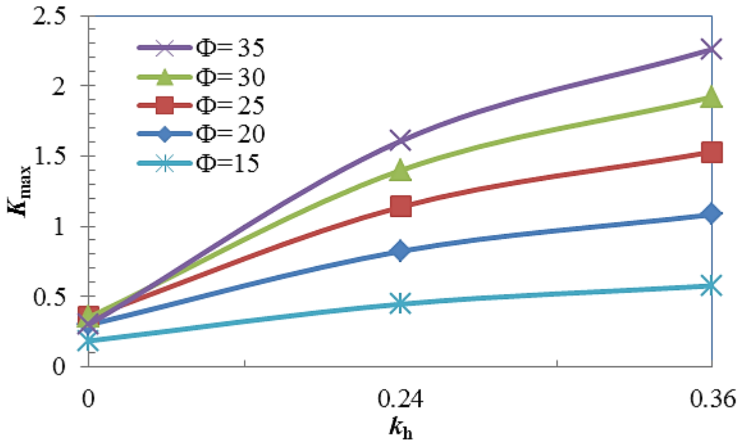

Figure 3. Changes of K_{max} with k_h for distinct value of ϕ and c^* = 0.33330, q^* = 0.55560, k_v = 0.12.

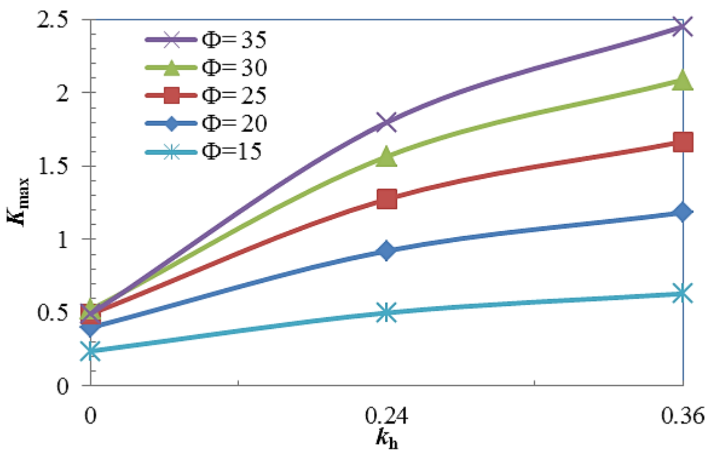

Figure 4. Changes of K_{max} with k_h for distinct value of ϕ and c^* = 0.33330, q^* = 0.55560, k_v = 0.18.

© STM Journals 2025. All Rights Reserved

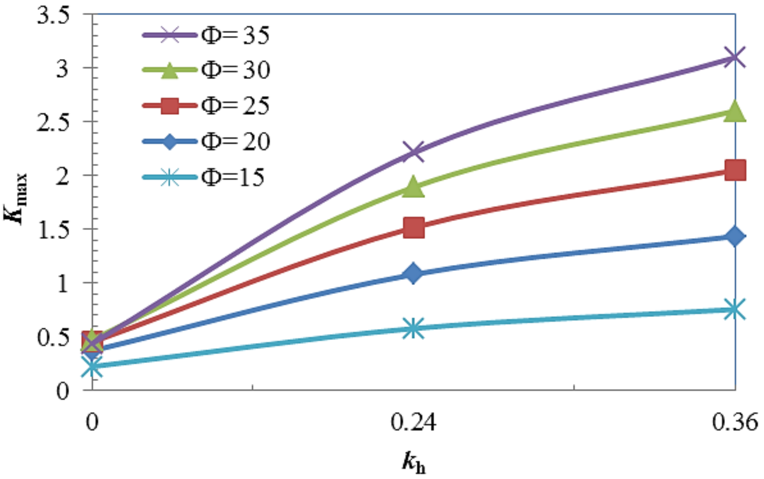

Figure 5. Changes of K_{max} with k_h for distinct value of ϕ and $c^* = 0.3333$, $q^* = 1.111$, $k_v = 0.12$.

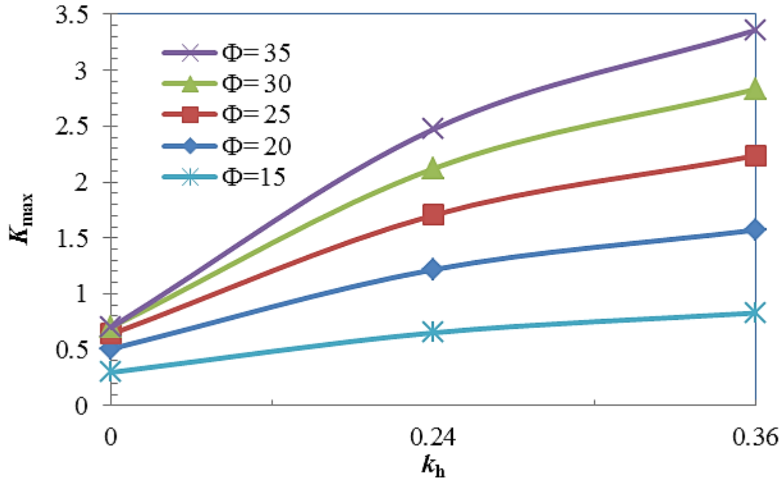

Figure 6. Changes of K_{max} with k_h for distinct value of ϕ and $c^* = 0.33330$, $q^* = 1.1110$, $k_v = 0.18$.

Impact of coefficient of cohesion (c) on K_{max}

From the fact that the absolute values of K_{max} are decreased for soil of cohesive nature, impact of k_v and the surcharge was more noticeable. Trends identified in Figs. (3-6) for $c^* = 0.33330$. Owing to a rise in cohesiveness, reinforcement force gratifying firmness is decreased also. As an example, for the case ($q^* = 1.1110$), the necessary K_{max} at ($k_h = 0.24, 0.36$), ($k_v = 0.12, 0.18$), $\phi = 30°$ is 0.4165, 0.5939 for respective values of k_h and k_v for $c^* = 0.3333$; which is 0.7639, 0.9413 for $c = 0$.

Impact of angle of frictional resistance (ϕ) on K_{max}

Impact of angle of shearing resistance (ϕ) on the values of K_{max}, is clearly shown by differences in Figures. (3-6). on increasing the worth of ϕ, K_{max} diminished for any specified worth of k_h and k_v. Impact of angle of frictional resistance (ϕ) is more noticeable when angle of frictional resistance is greater than 30°.

Impact of k_h, ϕ and surcharge loading (q) on α_{CR}

Variation in the failure plane's critical inclination (α_{CR}) with k_h for ($k_v = 0.50\ k_h$), and ϕ (20°, 25°, 30°, 35°, 40°, 45°), are shown in Figures. (7-8)for many pairs of dimensionless quantity (c^*, q^*). It is evaluated that the worth of $\alpha_{CR} = (45° + \phi/2)$ regarding the static situation. Furthermore, for any worth of k_h, the value of α_{CR} rises in tandem with the value of ϕ. Impact of ϕ can also be shown clearly for frictional resistance angles under 30°. For the case of dimensionless quantity ($c^* = 0.33330$, $q^* = 1.1110$) and $k_h = 0.24, 0.36$, the value of α_{CR} increased as 10.25%, 30.58% (for ϕ increases from 25° to 30°).

© STM Journals 2025. All Rights Reserved

Impact of c on α_{CR}

Impact of coefficient of cohesion of soil (c) on the worth of critical inclination α_{CR} is depicted in Figures. (7-8) α_{CR}, decreases as c^* increases. In Figs. (7-8) at surcharge ($q^* = 1.111$), for ($k_h = 0.24, 0.36$), angle of frictional resistance equal to 30°, the value of α_{CR} is 44.35°, 31.98° at ($c^* = 0.3333$).

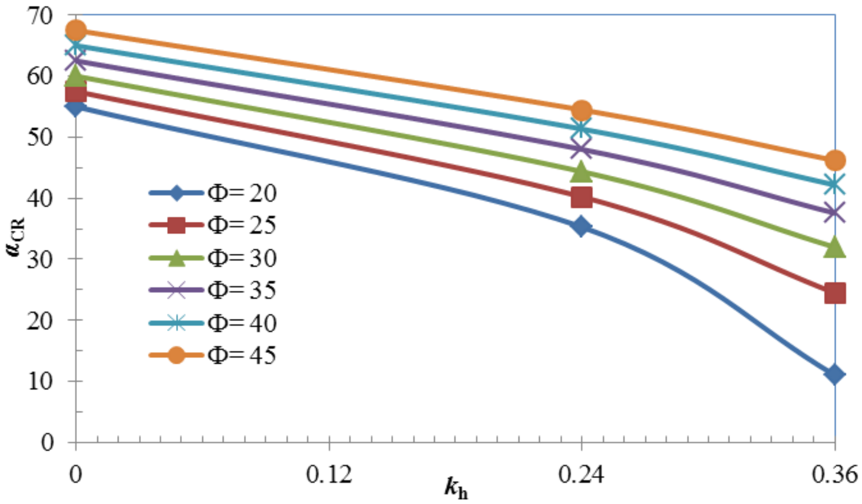

Figure 7. Changes of α_{CR} with k_h for c^* =0.33330, q^*=1.1110, $k_v = 0.12$.

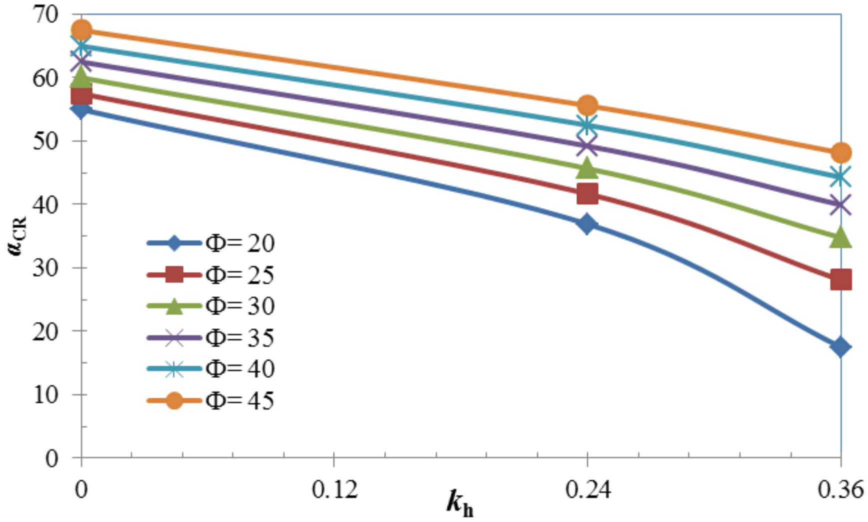

Figure 8. Changes of α_{CR} with k_h for c^* =0.33330, q^*=1.1110, $k_v = 0.18$.

Calculation of K_{max} at k_h= 0.36 and k_v = 0.18

For backfill soil are clayey sand (SC) of unit weight equal to 18000 N/m^3, soil cohesion equal to 8000 N/m^2, angle of shearing resistance equal to30°, reinforced soil wall of height equal to 8 m; outcomes by utilizing design charts for ($c^* = 0.33330$, $k_h = 0.36$, $k_v = 0.18$, $\phi = 30°$, $q^* = 1.1110$), $K_{max} = 0.7235$ and $\sum_{i=1}^{n} T_{i,\max} = \frac{1}{2}\gamma H^2 K_{\max} =$ 416.736 kN/m.

CONCLUSION

The key conclusions are as follows:

1. As the values of the horizontal seismic coefficients grow from 0.24 to 0.36, the K_{max} increases. However, as the (k_v) and the angle of frictional resistance (ϕ) increases, it decreases the maximum reinforcement force coefficient.
2. In reinforced soil wall's seismic design, the impact of the k_h is more noticeable than the k_v.

© STM Journals 2025. All Rights Reserved

3. As the k_h is rises from 0.24 to 0.36, α_{CR} of the failure plane substantially reduces.
4. At k_h = 0.36, the worth of α_{CR} is modified by the worth of soil cohesiveness rises.
5. When the worth of the (q) rises, the worth of α_{CR} of the failure plane also rises. Conversely, though, as the (q) are rises, the percent increase in the α_{CR} of the failure plane decreases due to increase in k_h from 0.24 to 0.36.

REFERENCES

1. Gupta A, Sawant VA. Simplified solution to analyse seismic stability of reinforced soil wall. International journal of geotechnical engineering. 2018 Dec 25.
2. Chandaluri VK, Sawant VA, Shukla SK. Seismic stability analysis of reinforced soil wall using horizontal slice method. International Journal of Geosynthetics and Ground Engineering. 2015 Sep;1:1-0.
3. Ahmadabadi M, Ghanbari A. New procedure for active earth pressure calculation in retaining walls with reinforced cohesive-frictional backfill. Geotextiles and Geomembranes. 2009 Dec 1;27(6):456-63.
4. Guler E, Hamderi M, Demirkan MM. Numerical analysis of reinforced soil-retaining wall structures with cohesive and granular backfills. Geosynthetics International. 2007 Dec;14(6):330-45.
5. Ling HI, Leshchinsky D, Perry EB. Seismic design and performance of geosynthetic-reinforced soil structures. Geotechnique. 1997 Oct;47(5):933-52.
6. Nouri H, Fakher A, Jones CJ. Development of horizontal slice method for seismic stability analysis of reinforced slopes and walls. Geotextiles and Geomembranes. 2006 Jun 1;24(3):175-87.
7. Deepankar C, Nimbalkar SS. Pseudo-dynamic approach of seismic active earth pressure behind retaining wall. Geotechnical and Geological Engineering. 2006 Oct 1;24(5).
8. Rowe RK, Soderman KL. An approximate method for estimating the stability of geotextile-reinforced embankments. Canadian Geotechnical Journal. 1985 Aug 1;22(3):392-8.
9. Basha BM, Basudhar PK. Pseudo static seismic stability analysis of reinforced soil structures. Geotechnical and Geological Engineering. 2010 Nov;28:745-62.
10. Ghosh S, Prasad Sharma R. Seismic active earth pressure on the back of battered retaining wall supporting inclined backfill. International Journal of Geomechanics. 2012 Feb 1;12(1):54-63.

© STM Journals 2025. All Rights Reserved